

This article was downloaded by:

On: 25 January 2011

Access details: *Access Details: Free Access*

Publisher *Taylor & Francis*

Informa Ltd Registered in England and Wales Registered Number: 1072954 Registered office: Mortimer House, 37-41 Mortimer Street, London W1T 3JH, UK



Separation Science and Technology

Publication details, including instructions for authors and subscription information:

<http://www.informaworld.com/smpp/title~content=t713708471>

The Prospects for Large-Scale Electrophoresis

Cornelius F. Ivory^a

^a DEPARTMENT OF CHEMICAL ENGINEERING, WASHINGTON STATE UNIVERSITY, PULLMAN, WASHINGTON

To cite this Article Ivory, Cornelius F.(1988) 'The Prospects for Large-Scale Electrophoresis', *Separation Science and Technology*, 23: 8, 875 — 912

To link to this Article: DOI: 10.1080/01496398808063143

URL: <http://dx.doi.org/10.1080/01496398808063143>

PLEASE SCROLL DOWN FOR ARTICLE

Full terms and conditions of use: <http://www.informaworld.com/terms-and-conditions-of-access.pdf>

This article may be used for research, teaching and private study purposes. Any substantial or systematic reproduction, re-distribution, re-selling, loan or sub-licensing, systematic supply or distribution in any form to anyone is expressly forbidden.

The publisher does not give any warranty express or implied or make any representation that the contents will be complete or accurate or up to date. The accuracy of any instructions, formulae and drug doses should be independently verified with primary sources. The publisher shall not be liable for any loss, actions, claims, proceedings, demand or costs or damages whatsoever or howsoever caused arising directly or indirectly in connection with or arising out of the use of this material.

The Prospects for Large-Scale Electrophoresis

CORNELIUS F. IVORY

DEPARTMENT OF CHEMICAL ENGINEERING
WASHINGTON STATE UNIVERSITY
PULLMAN, WASHINGTON 99164

INTRODUCTION

Electrophoresis is capable of resolving biological materials on the basis of differences in their molecular weights, electrophoretic mobilities, isoelectric points, or various combinations of these properties. At laboratory scale, these include some of the most powerful techniques available for the gentle purification of biologically active molecules. For instance, isoelectric focusing (IEF, see Table 1) can resolve proteins whose isoelectric points, *pIs*, differ by as little as 0.01 pH unit. Likewise, SDS-PAGE will routinely isolate a discrete spectrum of proteins whose molecular weights differ by less than 2%. Although electrophoretic separations are sometimes carried out under hostile conditions, e.g., low salt concentrations, denaturing detergents, or extreme pHs, the basic technique is inherently mild and is universally applicable to the detection and purification of solutes ranging in size from several ångströms to several microns. Because of this, electrophoresis is widely used in the natural sciences for both analytical and prepatative work.

The beginning of modern electrophoresis is clearly marked by the invention of a practical bench-top apparatus (Fig. 1) designed by Tiselius (1) for the analysis of serum proteins. At that time only three blood proteins had been isolated, albumin, globulin, and fibrinogen, but, using moving boundary electrophoresis (MBE) with Schlieren optics, he was able to resolve the globulin fraction into three distinct components, the α , β , and γ globulins. The difficulties involved in designing such equipment had been known for several decades, but this was the first apparatus to simultaneously overcome the problems of sample dispersion, overheat-

TABLE 1
Acronyms Used in This Paper

ZE	Zone electrophoresis
MBE	Moving bounding electrophoresis
ITP	Isotachophoresis
IEF	Isoelectric focusing
PAG	Polyacrylamide gel
PAGE	Polyacrylamide gel electrophoresis
SDS-PAGE	PAGE with SDS in buffer
DISC	Discontinuous electrophoresis
BSA	Bovine serum albumin
Hg	Bovine hemoglobin
IgG	γ -Immunoglobulin
RZE, RCFE	Recycle zone electrophoresis
RIEF	Recycle isoelectric focusing
RITP	Recycle isotachophoresis
CRAE	Continuous rotating annual El
CACE	Counteracting column El

ing, and natural convection which had previously hindered development. As such, it fostered a revolution in the application of electrophoresis to the purification and characterization of biomolecules.

The introduction of superior anticonvectant media such as filter paper (2), starch (3), agarose (4), and polyacrylamide gels (5) displaced the use of sand, ground glass, etc., and accelerated the routine laboratory use of electrophoresis. During this same period new procedures, such as isoelectric focusing (6) and isotachophoresis (7), were developed in

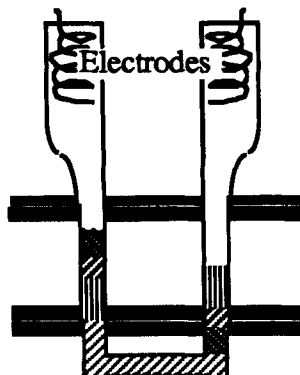


FIG. 1. Schematic of Tiselius' apparatus indicating final distribution of solute bands.

addition to zone and moving boundary electrophoresis, thereby increasing the resolution and range of electrokinetic separations. These methods have since been incorporated into highly specialized techniques such as two-dimensional (2-D) electrophoresis, originally performed on paper (8), which has evolved into the most powerful analytical technique for protein characterization available today. A modern protocol for 2-D electrophoresis utilizes IEF along one axis followed by SDS-PAGE along the second axis (9).

There are several popular techniques used for routine laboratory work with proteins. For instance, discontinuous gel electrophoresis (DISC), introduced independently by Ornstein (10) and Davis (11), uses a series of several gels with specialized buffers to load, stack, and separate solutes which have the same charge sign. Furthermore, there is a variation (12) of PAGE which involves the addition of denaturing anionic surfactant, SDS (sodium dodecylsulfate) in buffered electrolyte, to a polyacrylamide gel. In this system, proteins migrate at a rate determined by their molecular weights and can be accurately calibrated against marker proteins. DISC and SDS-PAGE were combined by Laemmli (13) into a procedure which allows rapid and precise characterization of solutes according to their molecular weights.

In the past two decades, many different versions of these basic laboratory procedures (14, 15) have been devised and new techniques, e.g., Western blots, gradient gels, etc., have been added so that it is impossible to summarize them all in the space available here. Although the procedures indicated above are very powerful, they are limited by loading considerations, heat removal, and dispersion to solute capacities of less than 1 mg protein. The intent of this paper is to identify the sources and characteristics of these impediments, to review the work which has been done to mitigate these problems so as to extend the capacity of electrophoretic separators, and, finally, to examine the potential impact of research currently underway in this area.

BASIC TYPES OF ELECTROPHORESIS

All of the techniques mentioned in the Introduction of this article can be grouped into four major categories: 1) zone electrophoresis, 2) moving boundary electrophoresis, 3) isotachophoresis, and 4) isoelectric focusing. Within these four categories there are many different procedures which can be used to optimize separation, but the underlying physics involved in each case can always be related back to one of these four

groups (Fig. 2). What follows is a brief description of each of the four modes of electrophoresis.

Zone Electrophoresis

In zone electrophoresis (ZE), a thin band of multicomponent solute is introduced into a buffered electrolyte solution and then subjected to an electric field until the various components in the band resolve themselves. Since the electrophoretic velocities of the components are proportional to the applied electric field strength, the separation of components increases in direct proportion to exposure time. Electrophoretic mobilities of proteins generally fall in the range $\mu \approx 0.1\text{--}1.0$ $(\mu\text{m} \cdot \text{cm})/(V \cdot \text{s})$, so experiments are carried out over the better portion of an hour. For analytical work, ZE is often performed in a thin cell several centimeters long.

Zonal separations may be performed in free or supported media, in slab or cylindrical geometry, with or without added detergent, and these techniques are generally used on the microgram scale as a test of sample heterogeneity or on the submilligram scale to purify a sample for further experimentation. Variations of zone electrophoresis are among the most common laboratory techniques and include popular examples such as horizontal slabs of agarose or starch, PAGE, SDS-PAGE, and gel gradient SDS-PAGE (14).

Moving Boundary Electrophoresis

In moving boundary electrophoresis (MBE), a semi-infinite sample band is loaded into the cell near one of the electrode compartments. For instance, if MBE analysis is to be carried out on a set of cations with different mobilities, the sample is loaded into the anodic electrolyte compartment. The cathodic portion of the cell is then filled with a *leading electrolyte*, i.e., one whose effective cationic mobility is greater than the fastest ionic components undergoing analysis. Under an applied current the leading electrolyte will remain ahead of the sample and tend to *sharpen* the interfacial boundary separating it from the fastest component in the sample (16, 17). Unlike zone electrophoresis, which can separate ionic species irrespective of their charge *sign*, MBE cannot separate cationic and anionic species simultaneously.

For instance, consider a sample containing five cations in solution with a common anion and with cationic mobilities, μ , ordered so that

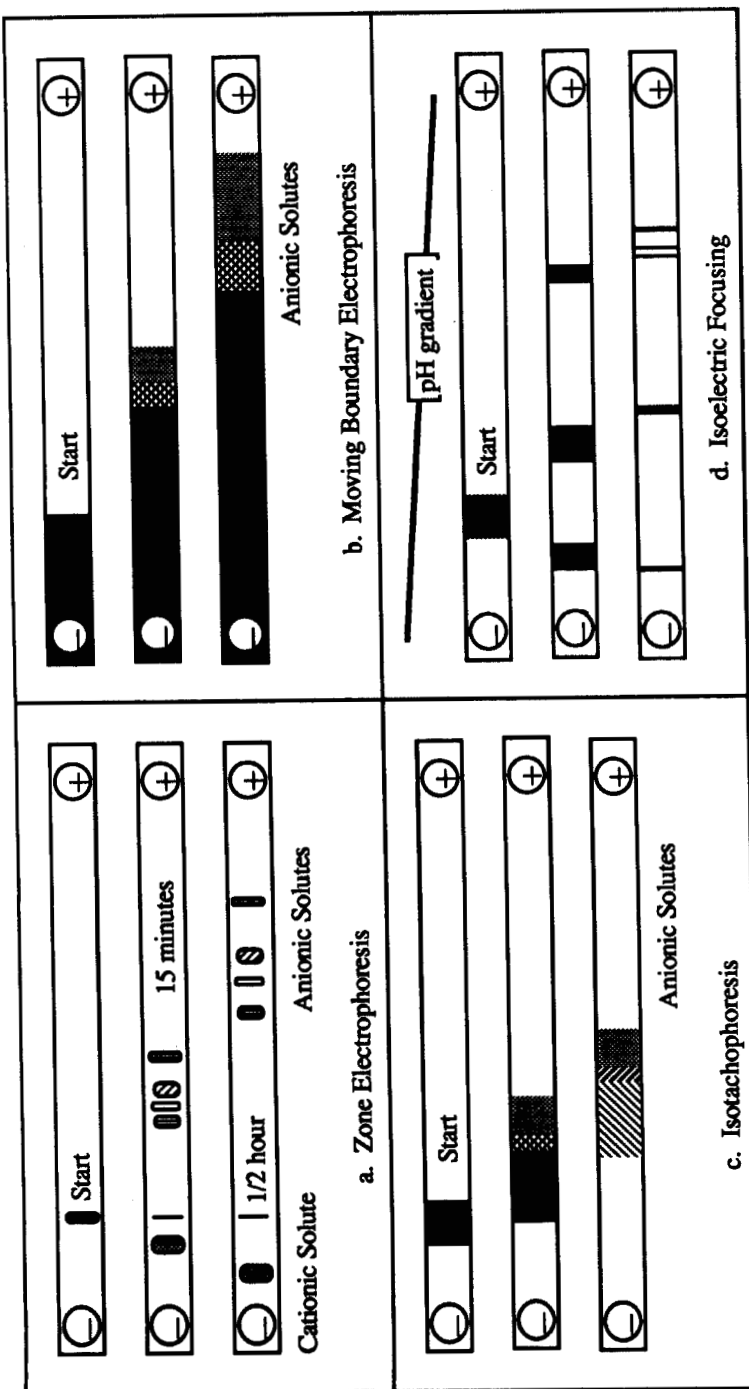


FIG. 2. The four basic modes of electrophoresis.

$$\mu_{LE} > \mu_1 > \mu_2 > \mu_3 > \mu_4 > \mu_5 > 0$$

When the electric field is turned on, the cations migrate across the cell toward the cathode and begin to separate into bands according to their mobilities. A band of pure Cation 1 forms behind the leading electrolyte, the length of this band growing linearly with time and its concentration strictly regulated by the current. Four more discrete bands will form behind the fastest cation, with each new phase containing the next fastest cation in addition to each of the cations in the leading bands. Thus, only the fastest solute is purified although the presence of each species can be detected and its mobility determined. The concentration of each cation remains constant within each band but differs between the bands. Any anionic species in the original sample are driven further into the anodic compartment and thus do not influence the formation or migration of the cationic bands.

Isotachophoresis

In isotachophoresis (ITP), a multicomponent sample with *finite* bandwidth is placed between two electrolytes; one with the properties of a leading electrolyte and the other with the properties of a trailing electrolyte, i.e., the effective mobility of the "training" ion is less than the mobility of the slowest ion in the sample. When current is applied, the components assemble themselves into N discrete, contiguous domains, each containing only *one* cationic species and separated by self-sharpening interfaces which move at the same velocity (17, 18).

Once again, the separated components order themselves according to their mobilities with the highest mobility phase leading and the lowest mobility phase trailing the sample bands according to the relation

$$\mu_{LE} > \mu_1 > \mu_2 > \mu_3 > \mu_4 > \mu_5 > \mu_{TE}$$

Once steady state is reached, the velocity and the phase concentrations depend in a complicated way on the mobility and ionic strength of the leading electrolyte phase. The ionic concentrations in the sample determine the component bandwidths while the conductivity difference between adjoining phases determines the extent of interfacial dispersion or mixing.

Isotachophoresis is well-suited to the analytical or preparative separation of homologous series of ions whose mobilities are sufficiently distinct that interfacial dispersion is not a problem. Examples of systems of ions on which isotachophoresis has been performed include the alkali

ions, organic ions, various heavy metal ions and ion complexes, peptides and nucleotides, and has been applied to enzymes and other proteins such as albumin and hemoglobin.

Isoelectric Focusing

Because most biological molecules are amphoteric in nature, their charge can vary from net positive at low pH to net negative at alkaline pH. A value of the pH therefore exists for which the molecule has a hypothetical mean charge of zero, and this is known as its *isoelectric point*. Since the net charge is zero at this point, the electrophoretic mobility is zero and, since virtually all biomolecules have distinct isoelectric points, a separation process can be envisioned in which each molecule migrates to its isoelectric point and then remains at that point (6, 19).

Since a negatively charged molecule will migrate toward the anode, the electrolyte in the anode compartment should be buffered at diminished pH so that as the molecule approaches the anode from the alkaline side, its charge will become less negative. The catholyte is buffered at elevated pH, and a stable pH gradient must be established across the electrophoresis chamber. An amphoteric molecule, e.g., protein, will migrate from any point in the cell with its net charge changing until it reaches its isoelectric point.

It is possible to establish the pH gradient either by electrolysis or by supplying acidic anolyte and basic catholyte as suggested above, but the resulting pH gradient might not be stable over the period of time required to complete the separation. There are, however, several techniques available for stabilizing the pH gradient, the most popular method involving the use of Ampholines (Biolyte, Servolyte) or other low molecular weight polyampholytes. These heterogeneous polymers distribute themselves throughout the cell by migrating to their individual isoelectric points and will thus establish and stabilize the pH gradient. Isoelectric focusing (IEF) is one of the most powerful methods for the characterization of biomolecules since it is capable of resolving solute bands with pIs which differ by less than 0.01 pH unit. It is also used for preparative purposes since even at larger loadings this technique will focus and separate bands with ΔpIs smaller than 0.1 pH unit.

COMMERCIAL ELECTROPHORESIS EQUIPMENT

Within a decade after Tiselius introduced his bench-top apparatus, research was underway to build a device which would conduct electrophoretic separations on a much larger scale. This earliest design (20)

consisted of a horizontal liquid film bounded below by a cathode and above by the anode, the cathode being cooled to stabilize the film against natural convection. Buffer was introduced through a multiplicity of ports distributed between the upper and lower electrodes at one end of the chamber and extracted through similar ports at the far end. Multi-component sample was introduced through a single port and fractionated as it passed between the electrodes. While some progress was made toward design of a commercial apparatus via this device, the problems cited earlier, and in particular natural convection, were not entirely overcome and this line of research was eventually abandoned.

This first attempt at large-scale electrophoresis is important not only for historical reasons but also because it set the stage for further development, introduced several key design features, and it drew attention to the most immediate obstacles hindering commercial development. Specifically, the separation could be carried out continuously and without the aid of anticonvectant media, but some other means would be required to stabilize the liquid film against natural convection. Furthermore, the electrodes would have to be isolated from the film to avoid disruption of the laminar flow by gas generation or denaturation of protein by contact with electrolysis products.

In the years that followed, many different approaches to hydrodynamic stabilization were tried: anticonvectant media (21), density gradient (22), viscous thickening agents (23, 24), magnetic rotation (25, 26), etc., and most of these attempts were successful in extending electrophoretic separation capacity. However, because they failed to resolve all of the problems facing large-scale operation simultaneously, these devices were never put into commercial service. The history and characteristics of several devices which are marketed commercially are given below.

The "Thin-Film" Apparatus

By the middle of this century, the problems associated with large-scale electrophoretic processing were well in hand and several continuous apparatuses had been demonstrated in Europe (27-29). These early devices consisted essentially of a pair of electrodes mounted on either side of a thin bed of porous material whose primary function was to provide an even flow of buffered, carrier fluid between the electrodes. Although sea sand, ground glass, and other materials had been used as anticonvectant media, the best results were obtained by using one or more sheets of filter paper. Scale-up entailed plying ever thicker sheaves

of porous paper together and, while natural convection was no longer an important consideration, overheating accompanied by solvent evaporation placed an upper bound on device loading.

Toward the end of that decade, Barrollier and coworkers (30) eliminated the need for anticonvectant media by switching to a thin (~0.5 mm), horizontal slit in which viscous forces stabilized the liquid film against natural convection. Both surfaces of this "free-flow" device were jacketed to remove Joule heat from the film, thus allowing use of higher electric field strengths and longer exposure of solutes to the field. This modification simplified cleaning and operation of the chamber, allowed a great measure of control over electroosmosis, and generally yielded more reproducible results than packed chambers.

During the next decade several companies, including General Electric, Beckman, Brinkman, Bender-Holbein, and Desaga, developed prototypes. Most of these chambers were designed so that the carrier fluid was introduced in a header at the top of the device, and feed was then injected into this stream through a fine capillary located at or just below the tops of the electrodes. As solute passes through the chamber, its components are displaced laterally via ZE. Individual solute components migrate in direct proportion to field strength so, when the resulting bands are sufficiently separated, they are collected at the effluent ports (31-37).

The vertical, jacketed column configuration (Fig. 3) with cocurrent flow, i.e., flow in the same direction as gravity, became the design of choice for a number of reasons. By 1970 preparative purification techniques including gel filtration, affinity chromatography, and ion exchange had outstripped the resolution and, in some cases, the capacity attainable by preparative free flow electrophoresis, so that only solutes which were subject to irreversible adsorption, sedimentation, or denaturation were targeted for separation by continuous electrophoresis. This subset of biomaterials includes a broad variety of members: prokaryotic and eucaryotic cells, red blood cells and lymphocytes, cell organelles, viruses, chromosomes, inclusion bodies, and membrane proteins (38-40), etc.

A horizontal slit, although it is insensitive to natural convection, is extremely sensitive to sedimentation, so a vertical configuration was adopted to allow purification of sedimenting particles. In a jacketed chamber, cocurrent flow allows somewhat greater throughput of sedimenting particles or concentrated solutes than countercurrent flow, i.e., in the direction opposite to gravity, and recovers more readily from occasional upsets due to thermal convection or gas bubbles.

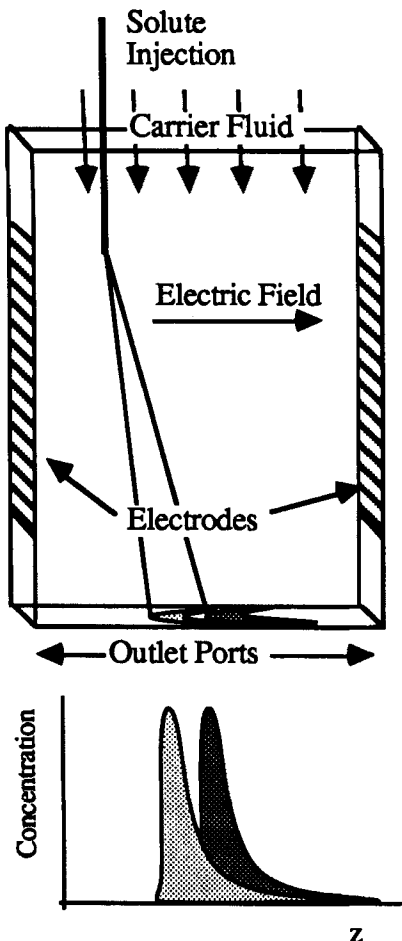


FIG. 3. Schematic of the vertical free-flow electrophoresis column.

Impediments to Large-Scale Processing: "Thin-Film" Apparatus

Throughput in the commercially available thin-film device operated in the ZE mode is generally limited to about 4 mL/h of 2% protein solution (36, 40) or about 0.1 g/h even under optimal conditions although it is possible to increase throughput by roughly one order of magnitude by changing the mode of operation (40) to IEF or ITP. Separations are conducted in buffered, free solution with conductivities below 10^{-2} mho/

cm to avoid excessive heat generation. In principle, one could raise device capacity by increasing the thickness of the film; however, this route to increased throughput is impeded by three obstacles: natural convection, overheating, and "crescent" dispersion.

As the thickness of the vertical CFE is increased, throughput rises with the square of the slit thickness. However, beyond a certain critical thickness which depends on the geometry of the device, the CFE exhibits a buoyancy instability which comes on with the *fourth* power of the transverse thickness and the second power of the electric field strength (41-43) as an indirect result of Joule heating. Under normal operating conditions this puts an effective upper limit of about 4 mm on the thickness of jacketed chambers, although in practice the slit thickness is typically 0.5-1.0 mm. The onset of unstable natural convection in the vertical chamber is characterized by the dimensionless parameter

$$\mathbf{Ra} \equiv \frac{g\beta|\nabla T| h^4}{\alpha v} \quad (1)$$

known as the Rayleigh number, where β is a thermal expansion coefficient, α is the thermal diffusivity, and v is the kinematic viscosity. In addition, $|\nabla T|$ is characteristic of the temperature gradient driving the flow, and h is the chamber slit thickness.

In a jacketed chamber with cocurrent flow, the column may become unstable when the Rayleigh number exceeds a value of π^4 (42). This occurs because buffer entering the column warms up as electric power is dissipated. The liquid expands slightly and creates a density inversion which then drives convection. At slightly supercritical Rayleigh numbers, researchers (44-46) have observed a stationary antisymmetric flow and a temperature pattern similar to the one predicted by Saville and Ostrach (42). If the Rayleigh number is increased further, a symmetric stationary pattern may appear, followed at higher \mathbf{Ra} by periodic and, eventually, chaotic (turbulent) motion which destroys the resolving power of the apparatus.

This barrier can be surpassed by modifying the design to a vertical-adiabatic-countercurrent flow configuration, a horizontal configuration (47), or by running the column in the reduced gravity of space (48-50). However, the next obstacle encountered is overheating of the solute since many proteins begin to denature rapidly at a temperature near 40°C. The temperature rise in the slit is determined using the thermal energy equation for an electrically heated cell,

$$k\nabla^2T + \mathbf{E} \cdot \mathbf{I} = 0 \quad (2)$$

where k is the thermal conductivity, \mathbf{I} is the current density, \mathbf{E} is the electric field, and where Ohm's law, $\mathbf{I} \equiv \sigma \mathbf{E}$, relates the current density to the electric field strength via the electrical conductivity. Assuming perfect cooling at the slit surfaces, the temperature rise in the center of the column is given approximately by

$$T - T_0 \approx \frac{1}{8} \frac{I_T \Delta \Phi h}{k L W} \quad (3)$$

where I_T is the total current, $\Delta \Phi$ is the potential difference between the electrodes, W is the electrode separation, and L is the chamber length. For an electric field of 100 V/cm and a fixed electrical conductivity of 0.001 mho/cm in aqueous electrolyte ($k \approx 0.005 \text{ W/cm}^\circ\text{C}$), the maximum transverse thickness permissible with a 40°C rise is about 8.5 mm. This allows increased throughput by a factor of $O(440)$ compared with a chamber thickness of 0.5 mm.

The temperature rise is further exacerbated by a phenomenon known as the *autothermal* effect (51) which causes the temperature to rise significantly higher than would be expected from the expression presented above. This occurs because the electrical conductivity of aqueous electrolyte solutions increases slightly with temperature. The warmer center of the slit dissipates more electrical energy than the cooler wall region, becomes slightly more conductive, and dissipates even more energy, thus amplifying the temperature rise in the core of the slit.

To estimate the magnitude of this effect, the thermal energy equation is rewritten to include, as a first approximation, a linear rise in the electrical conductivity with temperature:

$$k \frac{d^2T}{dy^2} + \sigma_0 E_0^2 + \left[\frac{d\sigma}{dT} \right]_{T_0} (T - T_0) E_0^2 = 0 \quad (4)$$

where the last term reflects the effect of the increased electrical conductivity. Solving this equation yields a centerline temperature rise:

$$T - T_0 \approx \frac{I_T \Delta \Phi h}{k W L} \frac{[1 - \cos(\lambda)]}{\lambda^2 \cos(\lambda)} \quad (5)$$

where

$$\lambda^2 = \left[\frac{d\sigma}{dT} \right]_{T_0} \frac{E_0^2 h^2}{k} \quad (6)$$

which predicts that the temperature will approach infinity as $\lambda \rightarrow \pi/2$ since $\cos(\lambda)$ vanishes in that limit. Again assuming a 40°C excursion and noting that, to a first approximation,

$$\frac{d \ln(\sigma)}{dT} \approx - \frac{d \ln(\eta)}{dT} \quad (7)$$

the maximum slit thickness is limited to less than 3.5 mm, engendering a substantial loss in scale. Whenever an electrophoretic chamber is susceptible to the autothermal effect, its impact on scale-up must be very carefully considered during column design.

Finally, device resolution suffers as a result of the intense convective and electroosmotic dispersion associated with the *crescent* phenomenon (52). Because the velocity profile in the "thin-film" device is parabolic, solutes nearer the transverse walls travel through the chamber more slowly than those at the center and are thus displaced further by the electric field, giving rise to a crescent-shaped band (Fig. 4) which stretches along the axis of the electric field in direct proportion to time. Diffusive spreading, which increases with the square root of time, is negligible for proteins in a slit thicker than about 0.5 mm, so crescent formation dominates dispersion in the CFE.

Electroosmosis (a.k.a. electroendoosmosis) is driven by the electrophoretic motion of double layer ions adjacent to solid surfaces with fixed charges. The surface charges are fixed in space so that only the mobile ions in the double layer can move under the action of the field. As they move they impart momentum to the solvent and thus accelerate the fluid near the fixed surface. Since the double layer contains a net number of charges equal and opposite to the charge on the fixed surface, electroosmotic flow is in the direction *opposite* to the electrophoretic velocity that the surface would have if it were free to move. In free solution, electroosmosis gives rise to a bulk flow which strongly affects the shape and width of the solute bands.

The bulk flow driven by electroosmosis is parabolic and appears to

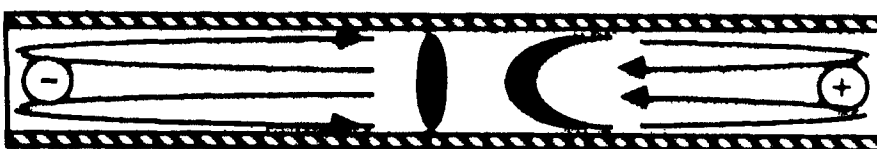


FIG. 4. Crescent formation due to electroosmosis in a closed, rectangular slit.

violate the "no-slip" condition over macroscopic length scales although this condition is satisfied within the electrical double layer. Strickler and Sacks (53) showed that this phenomenon can be used to eliminate crescent formation in the CFE by adjusting the ζ -potential of the slit surfaces.* It turns out that the optimal value of the slit surface ζ -potential is precisely that of the "key" component being separated, so it is generally beneficial to precoat the chamber surfaces with one of the solutes undergoing separation, if this coating is stable.

There are now several published models available for predicting concentration and flux profiles in the "thin-film" device. These include analytical expressions (54-56), numerical models (42, 57, 58) in the zero-diffusion limit, semianalytical expressions for finite but small diffusion coefficients (54, 59), and analytical expressions in the rapid diffusion regime (60). This last class of models can also be applied in the modeling of packed, nonporous beds.

Gobie (55) showed theoretically that bandwidths in a typical "thin-film" device will increase 10-100 times faster due to crescent dispersion than by diffusion. Bandwidth increases in direct proportion with time, and Hannig et al. (36) showed experimentally that this places an upper limit on the effective length and resolving power of a given column under prescribed operating conditions. This limitation can be mitigated to some extent by precoating the slit surfaces, by inducing a lateral crossflow of solvent, or by using serial electric fields; however, crescent dispersion eventually limits the resolution of the "thin-film" column.

Stress Stabilized Free-Flow Electrophoresis

In the late thirties Philpot (20) attempted to extend the scale of the U-tube (1) by adapting it to continuous separations. However, it was not until the mid-sixties that he finally designed a chamber (61) which achieved stable operation. This was accomplished by applying a transverse stress field across the thin annulus formed between two concentric cylinders, which house the electrodes, and then using the annulus as the separating chamber.

In this design the inner cylinder is fixed and generally serves as the cathode while the outer cylinder, which functions as the anode, rotates at

*The ζ -potential is the electrical potential measured at the surface of shear which is the interface separating the Gouy-Chapman ion cloud from the Stern layer of adsorbed ions and molecules. Adjusting the ζ -potential is equivalent to modifying the surface charge density.

speeds approaching 150 rpm, generating the stabilizing velocity gradient. Carrier fluid flows axially through the annulus, and feed is injected through a ring-shaped opening just below the electrodes (Fig. 5). This configuration allows operation at throughputs in excess of 1 L/h, three orders of magnitude greater than the "thin-film" device, which translates to more than 10 g/h of protein. A commercial version of this device is now available as the Biostream separator.

The design, construction, and operation of the Biostream unit is radically different from the "thin-film" apparatus. For instance, the carrier fluid in the Biostream chamber flows in the direction opposite to gravity in order to discourage unstable convection. The radial stress field gives added stability and damps stable convection driven by radial temperature gradients. In addition, the parabolic velocity profile of the carrier fluid is used to advantage to sharpen the solute bands during separation. Finally, because the electric field in the Biostream runs perpendicular to the transverse, annular surfaces, there is no electroosmosis and dispersion is, in principle, controlled by the much slower diffusive process (62-64).

Several models of solute behavior in the Biostream have been

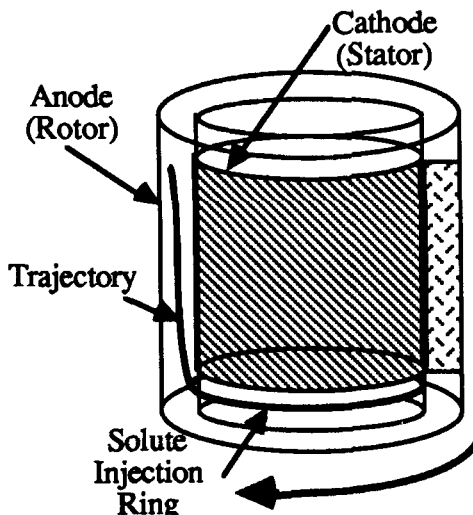


FIG. 5. Schematic of the Biostream separator. The rotor turns at about 150 rpm over the stator, generating a stabilizing velocity gradient. Solutes injected through the ring at the bottom of the annulus follow an S-shaped trajectory between the electrodes and elute through a series of ports (not shown) at the top of the column.

published (62, 65, 66) and, in theory, solute location in the annulus can be estimated using the simple trajectory equation

$$x - x_0 = \frac{\sigma Q}{\mu I_T} \left\{ 3 \left[\frac{r - a}{b - a} \right]^2 - 2 \left[\frac{r - a}{b - a} \right]^3 \right\} \quad (8)$$

where $x - x_0$ is the axial displacement of the solute band from the stator feed ring as it passes through the annulus, a is the stator radius, b is the rotor radius, and r is the radial position in the annulus. In addition, I_T is the total current passed and Q is the volumetric flow through the annulus. Band spreading or dispersion is computed as the standard deviation, χ , using the *Einstein* relation

$$\chi = \sqrt{2 \frac{D(x - x_0)}{U_{av}}} \quad (9)$$

where D is typically less than 10^{-6} cm²/s for proteins. Although this expression is not exact when applied to systems with parabolic flow profiles, it has been shown by comparison with solutions of the convective-diffusion equation (66) to give an excellent *theoretical* estimate of the dispersion.

Impediments to Large-Scale Processing: Biostream

Experiments (62, 65) indicate only qualitative agreement with theory since the dispersion measured in the apparatus is consistently found to be several times greater than predicted. The reasons for this departure from theory are not well understood but are thought to be either mechanical (65, 66) or physicochemical in nature. Although this does limit the range of application to systems in which "key" solutes have at least a 25% difference in mobility, a great many separations still fall into a category where the relatively large throughput compensates for mediocre resolution. In practice, one may require a 100% difference in mobilities to completely separate two solutes.

A more serious limitation arises because it is difficult if not impossible to remove dissipated electrical heat from the Biostream, essentially because the electrodes are located on the transverse surfaces. Because of this, the operator must rely on the high heat capacity of the solvent to control the axial temperature rise along the annulus. Ignoring transverse gradients, the temperature rise can be calculated from the thermal energy equation

TABLE 2
Protein Solubilities in Water (67)

Protein	Solubility (g/100 mL)	Temperature (°C)
Casein	0.011	25
Insulin	0.0009	5
Lactoglobulin	0.058	25
Equine serum albumin	1.10	0
Oxyhemoglobin	8.0	25

$$\rho C_p U_{av} \frac{dT}{dx} = \mathbf{I} \cdot \mathbf{E} \quad (10)$$

where ρ is the density and C_p the heat capacity of the electrolyte. Noting that the autothermal effect does not arise with this electrode configuration, integration yields a temperature rise

$$T - T_0 \approx \frac{I_T \Delta \Phi}{\rho C_p Q} \quad (11)$$

where I_T is the total current, $\Delta \Phi$ is the potential difference between the electrodes, and Q is the volumetric flow rate of carrier fluid. Typical values of the current and voltage used in the Biostream are 30–100 A and 30–60 V, which, with a volumetric flow rate in the range of 10 cm³/s, yields a temperature rise up to 40°C.

Another way to assess performance is to compute the maximum allowed value of the parameter, $E\sqrt{\tau}$, the product of the electric field strength and the square root of the holdup time. Inverting and rearranging Eq. (11), we find that

$$E\tau = \frac{EL}{U_{av}} = \sqrt{\rho C_p \Delta T \frac{L}{\sigma U_{av}}} \quad (12)$$

and noting that $\tau \approx L/U_{av}$, this can be written as

$$E\sqrt{\tau} = \sqrt{\frac{\rho C_p \Delta T}{\sigma}} \quad (13)$$

a parameter which is independent of device geometry. Assuming a conductivity of 0.001 mho/cm and a maximum temperature rise of 40°C, the upper limit on this parameter becomes

$$E\sqrt{\tau} \approx 500 \frac{\text{V}}{\text{cm}} \text{ s}^{1/2} \quad (14)$$

For a 1-min holdup time, this formula predicts that a maximum electric field of about 65 V/cm can be used without overheating the solutes. Noting that electrophoretic displacement is equal to

$$\Delta r = \mu Et \quad (15)$$

and that displacement to the center of the annulus in the Biostream is roughly 0.20 cm, the lower limit on the electrophoretic mobilities of solutes which can be processed through this device is approximately $1 \frac{(\mu\text{m} \cdot \text{cm})}{(\text{V} \cdot \text{s})}$, a fairly severe limitation. One might argue that this problem can be overcome by reducing the conductivity of the carrier fluid, but this can only go so far before the protein concentration surpasses its solubility limit or the device develops a conductive-dielectric instability, a phenomenon discussed in the next section. The lowest practical conductivity which could be used routinely is probably about 10^{-4} mho/cm, and it is reasonable to expect that the resolving power of this device will improve in inverse proportion to the conductivity. Thus, when it can be operated with dilute electrolyte, this apparatus should work fairly well.

In summary, the advantages of the Biostream are that it can process fairly concentrated protein feedstreams at a volumetric flow rate of several liters per hour or, in terms of protein feed, 10–100 g/h, which is about three orders of magnitude greater than the capacity of the "thin-film" device. This device is hydrodynamically stable and is not susceptible to electroosmosis or to the autothermal effect, but it suffers from anomalous dispersion of as yet unknown origin which limits resolution. Finally, because the device is necessarily adiabatic, a minimum mobility is established for fixed ionic strengths, below which the apparatus can be expected to perform poorly.

The Biostream has been very carefully designed to operate in a regime where many proteins can be purified by electrophoresis. However, because the device generally operates near its design limits, it is of the utmost importance that all separations be carefully planned before hand to check the feasibility, sensitivity to upset, and product resolution under realistic operating conditions. With proper planning this device should perform adequately.

TRENDS IN RESEARCH AND DEVELOPMENT

The remainder of this review focuses on several novel approaches to large-scale electrophoretic processing. The list of devices considered here is by no means comprehensive. In particular, it excludes electropolarization chromatography (69) and dielectrophoresis (70) which, although they both have shown promise, are not currently being considered for application to large-scale separations. On the other hand, the four processes described below have considerable potential to successfully alter the way electrophoresis will be performed at preparative and production scales.

Recycle Isoelectric Focusing (RIEF)

The application of recycle to continuous electrophoretic processing was pioneered by Bier (71) for IEF (Fig. 6). The heart of his apparatus is an adiabatic, multichannel slit which is partitioned into compartments by closely spaced, fine porosity nylon screens which act to damp convection but freely transmit macro-ions as they migrate in the electric field. During a run, each of the compartments develops a characteristic pH which is highest at the cathode and lowest at the anode and which changes sharply at the nylon mesh screens. Once a pH gradient is established, polyampholytic solutes are circulated continuously through the chamber until all components have migrated to their isoelectric points and a pseudoequilibrium is established. The electric field is then switched off and the apparatus and reservoirs are drained of product. Late model designs have eliminated the screens but use thinner slits to discourage lateral mixing.

The device is further stabilized by operating the chamber adiabatically and with carrier flow opposite to gravity to minimize unfavorable thermal gradients. Experiment and theory both indicate that, in this configuration, axial thermal gradients do not contribute significantly to unstable convection. Hence, only lateral concentration and temperature gradients, which may become large as the products focus into sharp bands, must be taken into account. In contrast to this, a vertical chamber in adiabatic operation with flow parallel to gravity is unstable under virtually all operating conditions.

Bier (72, 73) has been successful in producing several generations of RIEFs which have been designed for semibatch operation. Early models

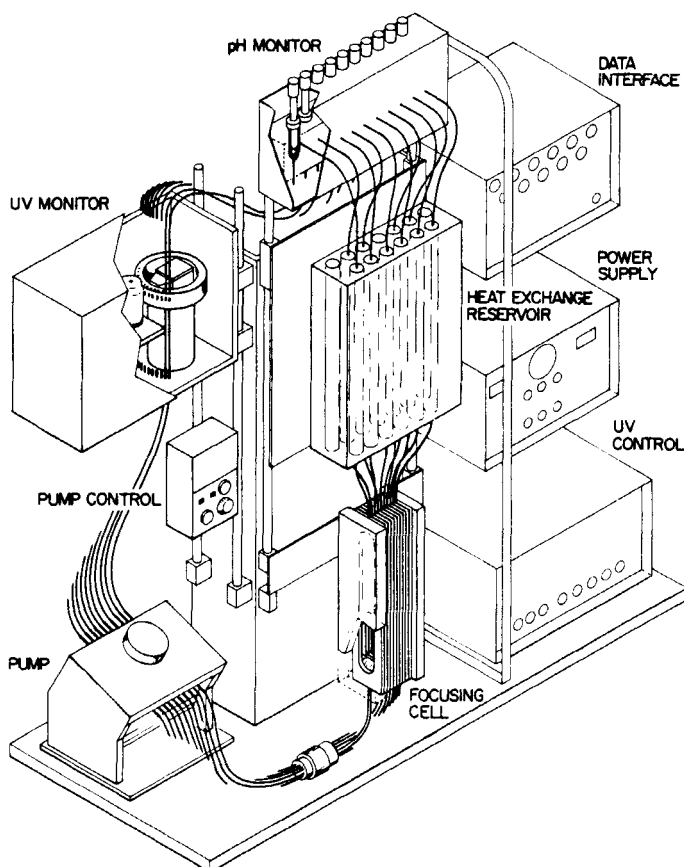


FIG. 6. The RIEF (72).

processed up to 2 g/h of protein by treating 2 L of feed containing 0.1% protein feed in 1 h. Later models have operated in the semibatch mode with charges in the neighborhood of 2 L/h, and so this equipment should be considered competitive with the Harwell apparatus in terms of volumetric throughput, marginally competitive in terms of protein mass processing rate, but far superior in terms of resolving power. In fact, it is expected that proteins whose *pIs* differ by as little as 0.1 pH unit can be completely resolved in this type of device.

Using recycle, the repeated contacting of solute with the electric field allows the separation to be brought arbitrarily close to completion before

solutes are eluted and the lower field strength reduces Joule heating so the temperature rise per cycle can be kept below 5°C. Because the system is modular, heat generated by electrical dissipation can be removed from the process streams via a multichannel heat exchanger located in the recycle circuit and the process streams may be monitored externally for temperature, pH, UV absorbance, etc.

The thermal and flow characteristics of the RIEF are similar to the "thin-film" device except that the low temperature rise precludes interference from the autothermal effect and the band sharpening associated with IEF mitigates crescent dispersion. However, solute behavior in IEF is entirely different from ZE. In zone electrophoresis, migration distance is proportional to time and the electrophoretic velocity is roughly constant so ZE is a rate-governed process. In isoelectric focusing, solutes migrate toward a fixed point where $\text{pH} \approx pI$ and then slowly sharpen into discrete bands, so IEF is an equilibration process.

By way of illustration, the band thickness at equilibrium can be estimated using the following, approximate model. First, assume that the pH gradient is linear near the isoelectric point and that the solute charge varies as

$$z \approx \left[\frac{d(z)}{d(\text{pH})} \right]_{\text{pH} = pI} (pI - \text{pH}) = \left[\frac{d(z)}{d(\text{pH})} \right] \left[\frac{d(\text{pH})}{d(x)} \right] x = -\gamma x \quad (16)$$

where the solute's pI is located at $x = 0$. The solute concentration obeys the Nernst-Planck equation

$$J_s \equiv -D_s \frac{dC}{dx} + \mu_s EC = 0 \quad (17)$$

where the latter equality holds if the band is stationary. Next, all ampholines are assumed stationary so that current is carried only by the supporting electrolyte which furnishes a background conductivity, σ^B , outside the solute band. Then, so long as the condition

$$C \ll \frac{\sigma^B}{|z| z_- \omega_s F} \quad (18)$$

is met at the isoelectric point and the solute does not precipitate, the concentration profile is symmetric about the pI and has a distribution given by

$$C \propto e^{-x^2/\kappa^2} \quad (19)$$

where the square of the lengthscale is

$$\kappa^2 \approx \frac{\sigma^2 D_s}{\beta \omega_s I} \quad (20)$$

in which $\omega_s \approx 10^{-5} \text{ cm}^2/(\text{coul} \cdot \text{V} \cdot \text{s})$ is the absolute mobility, $D_s \approx 10^{-6} \text{ cm}^2/\text{s}$ is the diffusion coefficient of the solute, and I is the current density. For typical values of these parameters, e.g., $\beta = 10$ charges per pH unit times 0.5 pH units per cm, a background conductivity of 10^{-3} mho/cm , and a current density of 10^{-3} A/cm^2 , the bandwidth scale factor is

$$\kappa \approx \frac{1}{\sqrt{50}} \text{ cm} \approx 0.2 \text{ mm} \quad (21)$$

The significance of this expression is that it correctly predicts that the product band will be sharpened by increasing the current, decreasing the background conductivity of the supporting electrolyte or decreasing the diffusivity of the solute, e.g., by using a tight mesh gel. However, the change in focused band thickness varies with the square root of the change in these parameters. The slope of the pH gradient can also be increased, but this will lead to an overall *drop* in resolution since the distance between neighboring bands decreases in direct proportion to the increase in the pH gradient while the band thickness decreases with the square root.

Another important consideration is the length of time it takes for a solute to focus. Once again this parameter can be readily estimated if a few simple assumptions are made. Consider a single solute molecule starting at a distance x from its isoelectric point. Assume that a linear pH gradient is already established and does not vary during the remainder of the run. The velocity of the solute is then given by

$$v_s = \frac{dx}{dt} = \mu E = z_s \omega_s E \quad (22)$$

where $z_s \approx -\gamma x$ near the *pI*. Integration yields

$$x = x_0 e^{-\gamma \omega_s E t} \quad (23)$$

where x_0 is the initial position of the molecule relative to its *pI*. The

amount of time required for the molecule to move to within 1% of its equilibrium position is approximately $5 \times \{\gamma\omega_s E\}^{-1}$. For typical values of these parameters, e.g., $\gamma \approx 5$, $\omega \approx 10^{-5}$, $E \approx 50$ V/cm, this formula predicts that, under these conditions, about 30 min exposure to the field is required to focus. A detailed numerical treatment of IEF as well as the other modes of electrophoresis has been presented elsewhere by Palusinski and coworkers (74-76).

Impediments to Large-Scale Processing: RIEF

The most important consideration during process design with the RIEF is the cost of the ampholytes. To control cost and quality, the user will have to synthesize these materials himself and an extra separation step will have to be added to the process to recover the ampholytes, which are expensive, from the product stream. It is also possible that, for clinical testing and for therapeutic application, even trace amounts of ampholytes will be forbidden by federal regulation. Efforts to circumvent this problem have centered on finding ampholine-free buffering systems which can be used to establish stable, linear pH gradients (77-79).

Another drawback endemic to isoelectric focusing is that protein solubilities are generally lowest near their *pI*, so focused proteins are susceptible to aggregation and precipitation (67, 68). This is further exacerbated by the low electrolyte concentrations, i.e., 10^{-2} - 10^{-3} M, generally used in isoelectric focusing, but this can be mitigated to some extent by adding solubilizing agents such as urea to the buffer. In addition, as the system comes to equilibrium with ampholines and proteins focusing at their respective points of net zero charge, there are few ions available to carry current so the conductivity drops by roughly one order of magnitude to its background value. If the conductivity drops sharply in a thin region, the column may destabilize via two different mechanisms, one controlled by thermal gradients and the other by gradients in the conductivity and dielectric susceptibility.

In the first case a hot spot forms in the region of high resistance and, if viscous forces are insufficient to stabilize it, the laminar flow may be distorted by natural convection. The second instability is far more dangerous and may occur whenever a gradient in the dielectric susceptibility is exposed to a moderate, e.g., 50 V/cm, electric field. At present, this instability is poorly understood but is almost certainly due to the conductive and dielectric gradients which accompany concentration gradients. This instability, which is related to a conductive instability

described by Hoburg and Melcher (80), can disperse solute over the entire chamber volume within a few seconds. Because IEF generates sharply focused product bands, as the process nears completion it may become particularly susceptible to this instability.

Despite these potential problems the RIEF has been used to purify a wide variety of biomaterials, especially proteins, including serum proteins, snake venom, etc., and this type of equipment will soon be commercially available for preparative work.

Recycle Continuous Flow Electrophoresis (RCFE, RZE)

Unlike RIEF, in which effluent is recycled directly overhead, in recycle zone electrophoresis the effluent streams are shifted by a distance, S , before reinjection at the inlet ports. This gives rise to an effective *counterflow* of solvent against the migration velocities of the solutes undergoing separation. The electric field is then adjusted so that the components split into two product streams. For a two-component feed, the slower moving component is carried downstream by the counterflow of solvent while the faster moving component migrates upstream at a lower effective velocity. There is a region near the feed port where the two solutes overlap, but theory (55, 56, 81, 82) predicts that both can eventually be collected in essentially pure form. In principle, any two solutes with different mobilities can be separated by proper adjustment of the electric field and the shift.

Solutes migrate at their adjusted effective velocities until they reach regenerator units on either side of the recycle section. In the regenerators the counterflow of solvent is altered by changing S to prohibit solute from migrating past the outlet port (Fig. 7). With proper design, complete separation can be achieved with virtually no loss of biological activity.

Separation can be carried out in native buffer with background conductivities approaching 0.01 mho/cm, so low protein solubility is not a problem. Electrical power requirements are kept low by using small electric fields, e.g., <25 V/cm, so temperature excursions during each pass are typically less than 5°C. Besides these advantageous characteristics, the RZE is hydrodynamically stable if operated adiabatically with flow antiparallel to gravity. Finally, because of the low electric fields used and the broad concentration gradients which accompany separation, this device is not susceptible to the dielectric instability encountered in IEF.

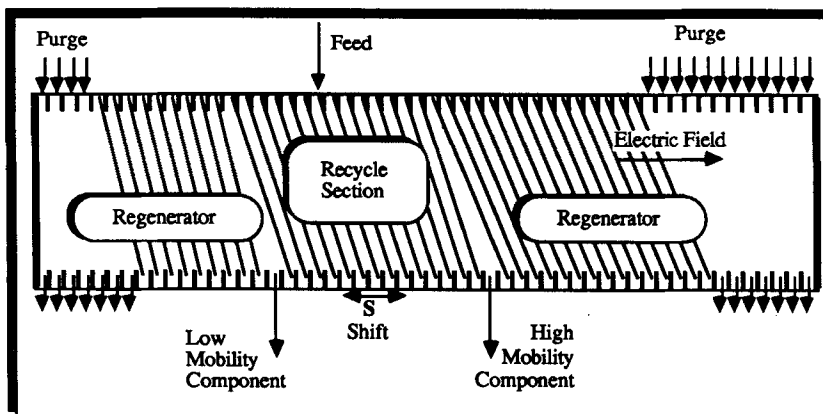


FIG. 7. The RCFE with regenerators.

Impediments to Large-Scale Processing: RZE

There are two major problems encountered with RZE. First, even though the transit time per pass is less than 1 min, the net holdup time is on the order of 1 h. During this time, if care is not taken to protect labile solutes from unfavorable conditions, they may be irreversibly inactivated by several different mechanisms, e.g., proteases. Second, in continuous operation the device will split a multicomponent feed into only two product streams so, if there are more than two important products in the feed, a "key" component must be chosen at which to make the cut, and offtake streams containing more than one product must then be sent for further processing. Modifications are currently being considered which may allow multicomponent purification and concentration in the RZE by semibatch processing.

Preliminary experiments on proteins using a prototype chamber with a 2-mm gap and 50 recycle ports indicate that the principles delineated in Gobie et al. (81) are obeyed in a qualitative sense. In one particular case a model feed mixture composed of nearly equal weights of bovine hemoglobin (Hg) and bovine serum albumin (BSA) in phosphate buffer at 5% mixed protein was processed continuously at 30 mL/h with a holdup time of about 1 h with a total power dissipation rate below 25 W. Each of the products was diluted by a factor of roughly three from its feed concentration, and neither showed any measurable cross-contamination

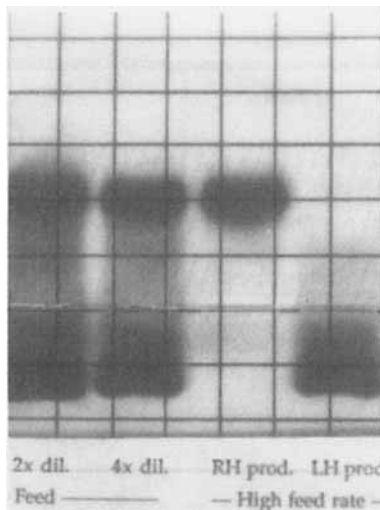


FIG. 8. Analysis by agarose gel electrophoresis of products from BSA-Hg separation in the RCFE. There is little detectable cross-contamination even at this high mass feed rate ≈ 1.5 g/h. Track 1: BSA-Hg feed mixture diluted 2 \times . Track 2: BSA-Hg feed mixture diluted 4 \times . Track 3: High mobility product, primarily BSA. Track 4: Low mobility product, primarily Hg.

in subsequent analysis by agarose gel electrophoresis (Fig. 8). Current efforts are directed toward increasing throughput in the apparatus while maintaining the high resolution obtained in these preliminary experiments.

Electrochromatography

An area which has recently experienced a sharp upsurge in interest combines the resolving power of electrophoresis with chromatography. When electrophoresis is performed in a bed of stabilizing media which may also have some specific absorption or adsorption properties, separation is affected by both electrophoretic and chromatographic phenomena, and device resolution can be dramatically improved by taking advantage of the interactions between the two processes.

The advantages of this combination are compelling: Consider, for instance, the purification by gel filtration chromatography on P-150 (Bio-Rad) beads of γ -globulin (IgG) in ascites fluid using a fixed column with length $L \approx 20$ cm and void fraction $\epsilon \approx 0.40$. For the sake of argument,

assume that the antibody is present at about 10% of total raw protein and the major contaminant in BSA, representing about 85% of the protein originally in the growth medium, in addition to the other soluble serum proteins and proteases exported from the hybridoma. In this gel the IgG has a K_{av} less than 0.05 and elutes from the column shortly after the void volume. By contrast the BSA, which has the highest molecular weight of the contaminating proteins, has a $K_{av} \approx 0.25$ but is present in high enough concentration that the IgG fraction appears as a shoulder on the leading edge of the BSA peak.

In this situation one would like to decrease the effective column velocity of the BSA relative to IgG so that it elutes as a separate peak. In the absence of an electric field the ratio of the elution velocities is approximately

$$\frac{V^{\text{BSA}}}{V^{\text{IgG}}} \approx \frac{\varepsilon + K_{av}^{\text{IgG}}(1 - \varepsilon)}{\varepsilon + K_{av}^{\text{BSA}}(1 - \varepsilon)} = 0.78 \quad (24)$$

However, if the column is run in 5 mM phosphate buffer at neutral pH, with a space velocity, εU , of 0.2 cm/min and an electric field of 20 V/cm (anode at inlet), this ratio changes to

$$\begin{aligned} \frac{V^{\text{BSA}}}{V^{\text{IgG}}} &\approx \frac{\varepsilon + K_{av}^{\text{IgG}}(1 - \varepsilon)}{\varepsilon + K_{av}^{\text{BSA}}(1 - \varepsilon)} \times \frac{\varepsilon U - \{\varepsilon + K_{av}^{\text{BSA}}(1 - \varepsilon)\}\mu^{\text{BSA}}E}{\varepsilon U - \{\varepsilon + K_{av}^{\text{IgG}}(1 - \varepsilon)\}\mu^{\text{IgG}}E} \\ &\approx 0.78 \times 0.81 = 0.63 \end{aligned} \quad (25)$$

Furthermore, if the electric field is doubled or the space velocity is cut in half, this reduces further to about 0.47, only slightly higher than the ratio computed for sucrose, ~ 0.43 . Therefore, under these conditions the BSA will come off the column when roughly one column volume has been passed. The IgG, on the other hand, will continue to elute with the void and can be collected, in principle, with no contaminating BSA.

In an early effort to demonstrate continuous electrochromatography, Vermuelen et al. (83, 84) constructed an annular column with a 10-cm outer radius, a 1.25-cm inner radius, a column length of 120 cm, and feed injected symmetrically from a ring at the base of the inner cylinder (Fig. 9). Two anticonvectant packings, 170-200 mesh glass beads and 100-150 mesh crosslinked polystyrene beads, were used to separate low molecular weight solutes. However, the resolution obtained in the separation of the amino acids glycine-glutamic acid and asparagine-proline was relatively poor, and interest in this approach slackened during the ensuing years. The low resolution was attributed to electroosmosis induced by the

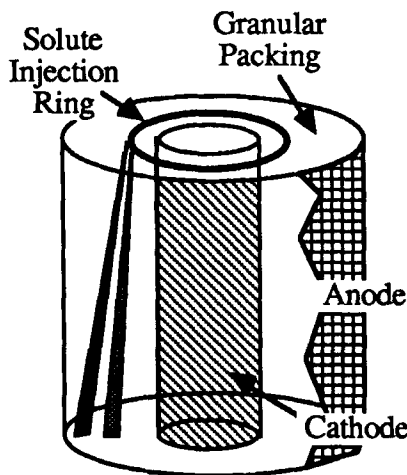


FIG. 9. Schematic of annular electrochromatograph after Vermeulen et al. (83).

electrode *diaphragms*, but the authors suggested that using thicker beds might improve the separating power of the device.

Recently, this general approach has been revived independently by Yoshisato et al. (85) and by Scott (86). The former group is developing an apparatus which they have named the CRAE (continuous rotating annular electrophoresis). In this device a thick annular bed is packed with inert or interactive media and the bed is rotated slowly, e.g., 0.005 rpm, about its axis. Multicomponent solute is introduced at a single point on the top of the bed and is carried axially through the device by an isocratic flow of solvent and azimuthally by rotation of the bed. An electric field is applied along the axis of flow in the annulus in a manner (Fig. 10) which preferentially retards or accelerates solutes to aid in their separation, and the products are drawn off through a multiplicity of ports located on the base of the annulus. This group has published an extensive theoretical analysis of the thermal and mass transport characteristics of the CRAE (85) and expect to have a unit in operation before the end of this year.

The research group at Oak Ridge entered this field by introducing electrodes between the packing and the cylindrical surfaces of their rotating annular chromatograph (87) and then removing heat into an ice bath located behind the outer electrode (Fig. 10). Because the chromatographic and electrophoretic processes are conducted along perpendicular axes, this approach has the potential to allow two-dimensional separa-

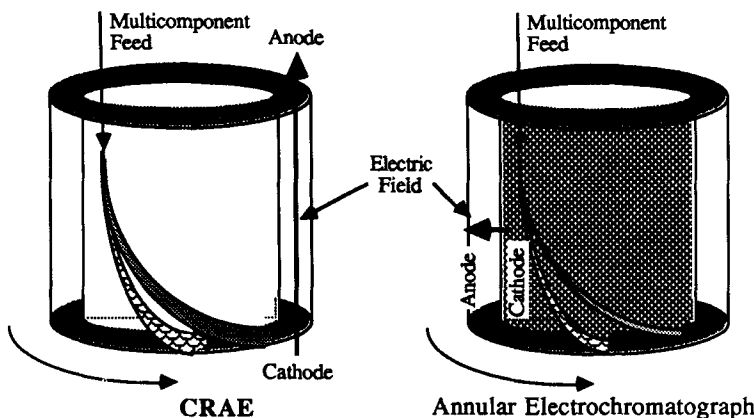


FIG. 10. Comparison of the rotating annular electrochromatographs of Yoshisato et al. (85) and Scott (86). Both chromatographs use slow rotation of the packed bed to allow continuous operation. Note, however, the difference in orientation of the electric fields in the two devices. In addition, the mechanism for withdrawing products from each of these chambers is markedly different (not shown). The CRAE has a single circular row of elution ports distributed around its base while the annular electrochromatograph withdraws products from four circular rows of ports.

tions, thus bringing extraordinary power and versatility to continuous bioprocessing if the apparatus can be made to function effectively. In principle there appears to be no reason why this approach cannot be made to work. However, preliminary experiments with bovine hemoglobin and blue dextran indicate that, in practice, this will not be a simple task.

Impediments to Large-Scale Processing: Electrophoresis

The major obstacle to large-scale electrochromatography is heat removal. Although the annular devices both resemble the Biostream wherein the high heat capacity of water moderates the temperature rise, low electrophoretic migration rates coupled with long chromatographic holdup times dictate that the temperature will rise until heat removal balances heat generation. Assuming a 40°C maximum temperature, perfectly conducting surfaces, a coaxial electric field of 20 V/cm, and an electrical conductivity of 0.001 mho/cm, the CRAE, which is susceptible to the autothermal effect discussed earlier (but not to the conductivity instability), is allowed a maximum characteristic slit thickness of about

1.5 cm. By comparison, the transverse electric field configuration used in the Oak Ridge electrochromatograph does not suffer from the auto-thermal effect (although it is susceptible to the conductive instability), so it admits a maximum slit dimension of about 4 cm if both surfaces are cooled or about 1 cm if only the outer surface is cooled. Taken in consideration with the slow chromatographic flow rates demanded by electrochromatography, these characteristic dimensions will allow significant, but not exceptional, increases in scale over commercial "thin-film" technology.

A second major obstacle, and about which much less is known, is dispersion. In addition to Taylor dispersion and the mechanical dispersion which normally accompanies liquid chromatography, there will be a contribution to the dispersion from electroosmosis both inside and outside the solid phase which, although it has the potential to sharpen solute bands, is more likely to increase dispersion. In addition to this, one must consider that liquid chromatography is most often carried out with buffer concentrations greater than 10 mM while electrophoresis is best performed at electrolyte concentrations below 10 mM. At these low salt concentrations the enormous surface area per unit volume of column packing is likely to generate appreciable nonspecific adsorption which will contribute significantly to the overall dispersion. This can perhaps be overcome as in IEF by adding nonconducting solubilizing agents if such agents do not interfere with the separation. Other lesser problems such as natural convection, thermal and electrical fluidization, and dielectric dispersion will also have to be tackled but it is expected that these phenomena will not greatly retard developments in this area.

When they are at last operational, this class of devices should offer many of the advantages of annular chromatography combined with the specificity of electrophoresis. Careful theoretical and experimental analysis of the fractionating power of these devices will be required to determine whether the potential of electrochromatography can be realized in practice, and it remains to be seen whether this approach can indeed overcome the excessive dispersion which hampered earlier experimental work.

Counteracting Chromatographic Electrophoresis (CACE)

An idea which is receiving a good deal of attention was recently proposed by O'Farrell (88). In his scheme a jacketed column is packed with two regions each made up from gel filtration media, e.g., BioGel or

Sephadex, with distinct K_{av} , of which one tends to exclude a target protein while the other tends to include that protein. If buffered solvent is then pumped *slowly* through the excluding region into the including region, a solute placed in the column will run through the excluding region at a relatively high velocity but will slow down in the including region because it spends more time inside the immobile gel phase.

If an axial current is applied across the column in a manner such that electrophoretic migration of the target protein proceeds against the flow of solvent, then a value of the electric field can be found which will allow the target protein to migrate to the interface between the two gels and halt there. A given range of electric field strengths will not only stop specific solutes but will also *concentrate* them at the interface between the gels. Solutes whose electrophoretic mobilities fall inside this range are retained at the interface while all other solutes are eluted either upstream or downstream of the interface (Fig. 11).

Using dilute electrochromatography theory and neglecting electroosmosis, we may readily estimate this range of mobilities to be

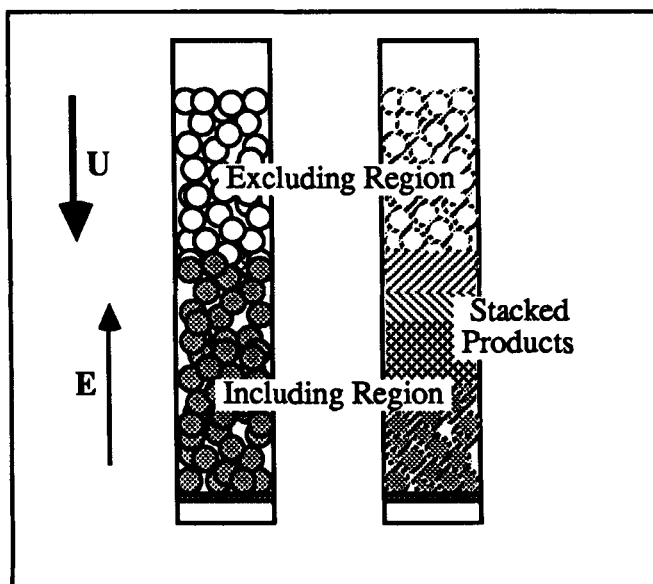


FIG. 11. Column electrochromatography (CACE) after O'Farrell (88). Note stacking of solutes at the interface in order of decreasing mobility.

$$\frac{\varepsilon^e U^e}{[\varepsilon^e + (1 - \varepsilon^e)K_{av}^e f^e]E^e} > \mu > \frac{\varepsilon^i U^i}{[\varepsilon^i + (1 - \varepsilon^i)K_{av}^i f^i]E^i} \quad (26)$$

where the superscript *e* refers to the properties of the excluding region while the superscript *i* refers to the including region. The parameter *f* is the ratio of the electrophoretic mobility in the gel phase to its mobility in the interstitial phase. This range can be adjusted to be very narrow or very broad by varying the properties of the media.

This technique has the important advantages of 1) being able to focus solute into a thin band *in native electrolyte* as opposed to isoelectric focusing which is performed near the protein's *pI* in a solution containing ampholytes, 2) being carried out in well-defined, inert media with common laboratory equipment, and 3) can be extended to batch capacities on the order of 1 g/run (88). Also, this apparatus can easily be modified for continuous operation. Throughputs on the order of 0.05 g/h have been achieved in a small diameter prototype unit (89) separating BSA from Hg.

Impediments to Large-Scale Processing: CACE

The CACE concept has several disadvantages including 1) that space velocities are limited by electrophoretic migration velocities and are extremely low, 2) throughput capacity is limited by heat transfer rates and this sets a limit on the column diameter of about 7 mm, 3) electric field strength is limited by buffer and electrolyte requirements, and 4) existing column filtration media are not optimally designed for use with this process. However, available media could be greatly improved and the resolving power of this technique dramatically enhanced by implementing simple changes in the physical and chemical properties of the media. In addition, limitations on scale associated with Joule heating can be eliminated by adding *interior* cooling coils to the apparatus. Since CACE focusing is an equilibration process, the coils would not contribute excessively to dispersion. With these comments in mind, there appears to be no practical limitation to the scale at which this technique can be applied.

Some theoretical work (90, 91) has already been published, and Hunter (92, 93) identified the applicable mass conservation equations and qualitatively described some of the anomalous phenomena which accompany use of discontinuous media in CACE. Several models and apparatuses are currently being used to study this technique, and over the

next 2 years important contributions are expected in this area including 1) advances in theory, 2) extension to continuous operation, and 3) development of superior focusing media.

CONCLUSION

Although development of preparative and industrial-scale electrokinetic separators has progressed slowly in the past, beginning in the late 1970s there has been a resurgence of interest and new ideas in this area. In addition to the two commercial devices currently on the market, there are several new routes to large-scale electrokinetic processing now under investigation which promise better resolution at higher throughputs than have been possible in the past. The keys to progress in this area are not only innovative thinking on the part of investigators, but detailed analyses of the bottlenecks restricting development, then careful testing of new ideas and equipment to establish practical principles for the design and operation of these columns.

NOTATION

a	inner radius of annulus
b	outer radius of annulus
C	concentration
C_p	heat capacity
D	diffusion coefficient
E	electric field strength
f	ratio of electrophoretic mobilities
g	gravitational acceleration
h	transverse slit or annulus thickness
I	current density
I_T	total current
J_s	solute flux
K_{av}	gel filtration partition coefficient
k	thermal conductivity
L	column length
pI	isoelectric point
Q	volumetric flow rate
r	radial coordinate in annulus
Ra	Rayleigh number

<i>S</i>	recycle shift
<i>T</i>	temperature
<i>t</i>	time
<i>U</i>	interstitial velocity in porous medium
<i>U_{av}</i>	average velocity
<i>V</i>	solute migration velocity in gel column
<i>x</i>	axial coordinate
<i>x₀</i>	axial location of feed ring
<i>y</i>	transverse coordinate
<i>z</i>	lateral coordinate
<i>z_i</i>	ionic valence

Greek Symbols

α	thermal diffusivity
β	thermal expansion coefficient
γ	charge gradient in IEF
ϵ	void fraction
Φ	electric potential
η	viscosity
ζ	zeta potential
κ	characteristic dimension of focused band in IEF
λ	dimensionless parameter defined in Eq. (6)
μ	electrophoretic mobility
μ_{LE}	electrophoretic mobility of leading ion
μ_{TE}	electrophoretic mobility of terminating ion
ν	kinematic viscosity
ρ	density
σ^B	background conductivity
σ	electrical conductivity
τ	holdup time in Biostream annulus
χ	standard deviation
ω_s	absolute mobility

Subscripts

<i>av</i>	transverse averaged
<i>LE</i>	leading electrolyte
<i>0</i>	characteristic parameter

<i>s</i>	solute
<i>T</i>	total or net
<i>TE</i>	trailing electrolyte
\pm	cation or anion

Superscripts

BSA	bovine serum albumin
<i>e</i>	excluding region of CACE column
<i>i</i>	including region of CACE column
IgG	γ -immunoglobulin

Acknowledgments

My thanks go to Dr. William Gobie for his helpful discussions and calculations and to Prof. Albert Wimmer for his translation into English of articles originally written in German. In addition, I am indebted to Dr. R. Yoshisato for his careful reading of and helpful suggestions in the preparation of this manuscript.

REFERENCES

1. A. Tiselius, *Trans. Faraday Soc.*, **33**, 524 (1937).
2. D. von Klobusitsky and P. Konig, *Arch. Exp. Path. Pharmakol.*, **192**, 271 (1939).
3. P. Consden, A. Gordon, and A. Martin, *Biochem. J.*, **38**, 224 (1944).
4. S. Hjerten, *Methods Biochem. Anal.*, **9**, 193 (1962).
5. S. Raymond and V. J. Wang, *Anal. Biochem.*, **1**, 39 (1960).
6. H. Svensson, *Arch. Biochem. Biophys. Suppl.*, **1**, 132 (1962).
7. F. M. Everaerts, J. L. Beckers, and Th. P. E. M. Verheggen, in *Isotachophoresis: Theory, Instrumentation and Applications*, Elsevier, Amsterdam, 1976.
8. E. L. Durrum, *J. Colloid Sci.*, **6**, 274 (1951).
9. P. H. O'Farrell, *J. Biol. Chem.*, **250**, 4007 (1975).
10. L. Ornstein, *Ann. N. Y. Acad. Sci.*, **121**, 321 (1964).
11. B. J. Davis, *Ibid.*, **121**, 404 (1964).
12. A. L. Shapiro, E. Viñuela, and J. V. Maizel, *Biochem. Biophys. Res. Commun.*, **28**, 815 (1967).
13. U. K. Laemmli, *Nature*, **227**, 680 (1970).
14. B. D. Hames and D. Rickwood (eds.), *Gel Electrophoresis of Proteins. A Practical Approach*, IRL Press, Washington, D.C., 1981.
15. A. T. Andrews, *Electrophoresis: Theory, Techniques, and Biochemical and Clinical Applications*, Clarendon Press, Oxford, 1986.
16. L. G. Longsworth, in *Electrophoresis* (M. Bier, ed.), Academic, New York, 1959.

17. F. M. Everaerts, F. E. P. Mikkers, and Th. P. E. M. Verheggen, *Sep. Purif. Methods*, 6(2), 287 (1977).
18. F. E. P. Mikkers and F. M. Everaerts, *Analytical Chemistry Symposium Series*, Vol. 6 (F. M. Everaerts, F. E. P. Mikkers, and Th. P. E. M. Verheggen, eds.), Elsevier, New York, 1981.
19. O. Vesterberg, in *Methods in Enzymology*, Vol. 22 (W. B. Jakoby, ed.), Academic, New York, 1971.
20. J. St. L. Philpot, *Trans. Faraday Soc.*, 39, 38 (1940).
21. H. G. Kunkel and R. Trautman, in *Electrophoresis* (M. Bier, ed.), Academic, New York, 1959.
22. H. C. Mel, *J. Theor. Biol.*, 6, 159 (1964).
23. Dobry and Finn, *Chem. Eng. Prog.*, 54(4), 59 (1958).
24. R. K. Finn, in *Separation Techniques* (H. Schoen, ed.), New York, 1962.
25. A. Kolin and S. J. Luner, *Anal. Biochem.*, 30, 111 (1969).
26. A. Kolin, *J. Chromatogr.*, 26, 164, 180 (1967).
27. H. Svensson and I. Brattsten, *Ark. Kemi*, 1(47), 401 (1949).
28. W. Grassmann, *Angew Chem.*, 62(7), 170 (1950).
29. W. Grassmann and K. Hannig, *Naturwissenschaften*, 37, 397 (1950).
30. J. Barrollier, E. Watzke, and H. Gibian, *Z. Naturforsch.*, 13b, 754 (1958).
31. H. Peeters, P. Vuylsteke, and R. Noe, *J. Chromatogr.*, 2, 308 (1959).
32. M. Bier, in *Electrophoresis* (M. Bier, ed.), Academic, New York, 1959.
33. A. Strickler, *Sep. Sci.*, 2(3), 335 (1967).
34. K. Hannig, in *Methods in Microbiology* (J. R. Norris and D. W. Ribbons, eds.), Academic, New York, 1971, Vol. 5B, p. 513.
35. Z. Prusik, in *Electrophoresis: A Survey of Techniques and Applications* (J. Chromatogr. Library, Z. Deyl, ed.), Elsevier, Amsterdam, 1979.
36. K. Hannig, H. Wirth, B.-H. Meyer, and K. Zeiller, *Hoppe-Seyler's Z. Physiol. Chem.*, 356, 1220 (1975).
37. R. Zeiller, K. Löser, G. Pasher, and K. Hannig, *Ibid.*, 356, 1225 (1975).
38. K. Hannig, in *Modern Separation Methods of Macromolecules and Particles*, Vol. 2 (Th. Gerritsen, ed.), Wiley, 1969.
39. K. Hannig, in *Techniques of Biochemical and Biophysical Morphology*, Vol. 1 (D. Glick and R. Rosenbaum, ed.), Wiley, 1972.
40. R. A. Mosher, W. Thormann, N. B. Egen, P. Couasnon, and D. S. Sammons, in *New Directions in Electrophoretic Methods* (J. W. Jorgenson and M. Phillips, eds.), American Chemical Society, Washington, D.C., 1987.
41. S. Ostrach, *J. Chromatog.*, 140, 187 (1977).
42. D. A. Saville and S. Ostrach, Final Report, Contract #Nas-8-31349 Code 361 (1978).
43. D. A. Saville, *Physicochem. Hydron.*, 2, 893 (1977).
44. P. H. Rhodes, NASA Tech. Memo. NASA TM-78178 (1979).
45. P. H. Rhodes and R. N. Snyder, in *Materials Processing in the Reduced Gravity Environment of Space* (G. E. Rindone, ed.), Elsevier, Amsterdam 1982.
46. C. F. Ivory, W. A. Gobie, J. B. Beckwith, R. Hergenrother, and M. Malec, *Science*, In Press.
47. R. S. Turk and C. F. Ivory, *Chem. Eng. Sci.*, 39(5), 851 (1984).
48. J. A. Gionnovario, R. N. Griffin, and E. L. Gray, *J. Chromatogr.*, 153, 329 (1978).
49. C. F. Ivory, *Electrophoresis*, 2, 31 (1981).
50. P. H. Rhodes, NASA Tech. Memo. NASA TM-78158 (1978).
51. E. Lynch and D. A. Saville, *Chem. Eng. Commun.*, 9, 201 (1981).
52. A. Strickler and T. Sacks, *Prep. Biochem.*, 3(3), 269 (1973).

53. A. Strickler and T. Sacks, *Ann. N. Y. Acad. Sci.*, **209**, 497 (1973).
54. C. F. Ivory, *J. Chromatogr.*, **195**, 165 (1980).
55. W. A. Gobie and C. F. Ivory, in *Separation, Recovery, and Purification in Biotechnology* (J. A. Asenjo and J. Hong, eds.), American Chemical Society, Washington, D.C., 1986, p. 169.
56. W. A. Gobie, PhD Thesis, University of Notre Dame, 1987.
57. P. H. Krumrine, PhD Thesis, Lehigh University, 1978.
58. P. Vaughn, PhD Thesis, Lehigh University, 1983.
59. J. F. G. Reis, E. N. Lightfoot, and H.-L. Lee, *AIChE J.*, **20**(2), 362 (1974).
60. C. F. Ivory, W. A. Gobie, and R. S. Turk, *Electrophoresis '83*, p. 293 (1984).
61. J. St. L. Philpot, in *Methodological Developments in Biochemistry*, Vol. 2, *Preparative Techniques* (E. Reid, ed.), Longmans, England, 1973.
62. P. Mattock, G. F. Aitchison, and A. R. Thompson, *Sep. Purif. Methods*, **9**(1), 1 (1980).
63. A. R. Thompson, *J. Chem. Tech. Biotechnol.*, **34B**, 190 (1984).
64. A. R. Thompson, in *Electrophoretic Techniques* (C. F. Simpson and M. Whittaker, eds.), Academic, New York, 1983.
65. P. T. Noble, *Biotech. Prog.*, **1**(4), 237 (1985).
66. J. B. Beckwith and C. F. Ivory, *Chem. Eng. Commun.*, In Press.
67. E. Cohn and J. T. Edsall, *Proteins, Amino Acids and Peptides*, Reinhold, New York, 1943.
68. C. Tanford, *The Physical Chemistry of Macromolecules*, Wiley, New York, 1961.
69. P. T. Noble, A. S. Chiang, T. A. Ugulini, and E. N. Lightfoot, *Sep. Sci. Technol.*, **16**(6), 619 (1981).
70. H. Pohl, in *Methods of Cell Separation* (N. Catsimpoolas, ed.), Plenum, New York, 1977.
71. M. Bier and N. B. Egan, in *Developments in Biochemistry*, Vol. 7 (Haglund, Westerfield and Ball, eds.), Elsevier-North Holland, Amsterdam, 1979.
72. M. Bier, in *Separation, Recovery, and Purification in Biotechnology* (J. Asenjo and J. Hong, eds.), American Chemical Society, Washington, D.C., 1986.
73. M. Bier, N. B. Egan, G. E. Twitty, R. A. Mosher, and W. Thormann, in *Chemical Separations*, Vol. I (C. J. King and J. D. Navratil, eds.), Litarvan Literature, Denver, Colorado, 1986.
74. M. Bier, O. A. Palusinski, R. A. Mosher, and D. A. Saville, *Science*, **219**(4590), 1281 (1983).
75. D. A. Saville and O. A. Palusinski, *AIChE J.*, **32**(2), 207 (1986).
76. O. A. Palusinski, A. Graham, R. A. Mosher, M. Bier, and D. A. Saville, *Ibid.*, **32**(2), 215 (1986).
77. M. Bier, R. A. Mosher, and O. A. Palusinski, *J. Chromatogr.*, **211**, 313 (1981).
78. O. A. Palusinski, M. Bier, and D. A. Saville, *Biophys. Chem.*, **14**, 389 (1981).
79. O. A. Palusinski, T. T. Allgyer, R. A. Mosher, M. Bier, and D. A. Saville, *Ibid.*, **13**, 193 (1981).
80. J. F. Hoburg and J. R. Melcher, *Phys. Fluids*, **20**(6), 903 (1977).
81. W. A. Gobie, J. B. Beckwith, and C. F. Ivory, *Biotechnol. Prog.*, **1**(1), 60 (1985).
82. W. A. Gobie and C. F. Ivory, *AIChE J.*, Submitted.
83. T. Vermeulen, L. Nady, J. M. Kroccta, E. Ravoo, and D. Howery, *Ind. Eng. Chem., Process Des. Dev.*, **10**(1), 91 (1971).
84. R. M. Hybarger, C. W. Tobias, and T. Vermeulen, *Ibid.*, **2**(1), 65 (1963).
85. R. A. Yoshisato, L. M. Korndorf, G. R. Carmichael, and R. Datta, *Sep. Sci. Technol.*, **21**(8), 727 (1986).
86. C. D. Scott, *Ibid.*, **21**(9), 905 (1986).

87. R. M. Canon, J. M. Begovich, and W. G. Sisson, *Ibid.*, 15, 655 (1980).
88. P. H. O'Farrell, *Science*, 227(4694), 1586 (1985).
89. C. F. Ivory and W. A. Gobie, Presented at the *Symposium on Recent Advances in Separation Techniques: Biochemical Separations*, AIChE Annual Meeting, New York, 1987.
90. B. J. McCoy, in *Chemical Separations*, Vol. I (C. J. King and J. D. Navratil, eds.), Litarvan Literature, Denver, Colorado, 1986.
91. B. J. McCoy, *AIChE J.*, 32(9), 1570 (1986).
92. J. B. Hunter, Presented at the *Symposium on Advances in Biological Separation Technology*, ACS National Meeting, Anaheim, California, 1986.
93. J. B. Hunter, *Sep. Sci. Technol.*, 23, 913 (1988).